DELPHI Collaboration

DELPHI 2001-048 CONF 476
07 July, 2001

Determination of A_{FB}^{b} using inclusive charge reconstruction and lifetime tagging at LEP1

K.Münich[1], M.Elsing[2], W.Liebig[1], B.Schwering[3], T.Allmendinger[4], G.Barker[4], M.Feindt[4], C.Haag[4], T.Scheidle[4]

Abstract

A novel method is used to measure the b quark forward-backward asymmetry at the Z pole on a sample of $2.80 \cdot 10^6$ hadronic events collected with the DELPHI detector in 1992 to 1995. An enhanced impact parameter tag is applied to the data to obtain a high purity b sample. For each event hemisphere the charge of the corresponding quark or anti-quark is determined using a neural network tag which combines in an optimal way the full available charge information from the vertex charge, the jet charge and from identified leptons and hadrons. The probability of correctly identifying b quarks and anti-quarks is calibrated on the data themselves comparing the rates of double hemisphere tagged like-sign and unlike-sign events. The b quark forward-backward asymmetry is determined from the differential asymmetry, taking small corrections due to hemisphere correlations and background contributions into account. The result is:

$$A_{FB}^{\mathrm{b}}\ (91.234\ \mathrm{GeV}) \quad = \quad 0.0967 \pm 0.0036(\mathrm{stat.}) \pm 0.0021(\mathrm{syst.})$$

Contributed Paper for EPS HEP 2001 (Budapest) and LP01 (Rome)

[1]Fachbereich Physik, University of Wuppertal, Postfach 100 127, D-42097 Wuppertal, Germany
[2]CERN, CH-1211 Geneva 23, Switzerland
[3]I.Physikalisches Institut, RWTH Aachen, Sommerfeldstrasse 14, D-52056 Aachen, Germany
[4]Institut für Exp. Kernphysik, Universität Karlsruhe, Postfach 6980, D-76128 Karlsruhe, Germany

1 Introduction

The measurements of the b quark forward-backward asymmetry at the Z pole provide the most precise determination of $\sin^2\theta^{\ell}_{\rm eff}$ at LEP. For pure Z exchange and to lowest order the forward-backward pole asymmetry of b quarks, $A^{0,\rm b}_{FB}$, can be written in terms of the vector and axial-vector couplings of the initial electrons $(v_{\rm e}, a_{\rm e})$ and the final b quarks $(v_{\rm b}, a_{\rm b})$:

$$A^{0,\rm b}_{FB} = \frac{3}{4}\frac{2a_{\rm e}v_{\rm e}}{a^2_{\rm e}+v^2_{\rm e}}\frac{2a_{\rm b}v_{\rm b}}{a^2_{\rm b}+v^2_{\rm b}} \tag{1}$$

Higher order electroweak corrections are taken into account by means of an improved Born approximation [1], which leaves the above relation unchanged, but defines the modified couplings ($\bar{a}_{\rm f}$, $\bar{v}_{\rm f}$) and an effective mixing angle $\theta^{\rm f}_{eff}$:

$$\frac{\bar{v}_{\rm f}}{\bar{a}_{\rm f}} = 1 - 4|q_{\rm f}|\sin^2\theta^{\rm f}_{eff} \tag{2}$$

using the electric charge $q_{\rm f}$ of the fermion. The b quark forward-backward asymmetry determines the ratio of these couplings. Therefore it is basically sensitive to $\sin^2\theta^{\ell}_{\rm eff}$ defined by the ratio of the electron couplings.

Previously established methods to measure the b quark forward-backward asymmetry in DELPHI [2, 3] were either exploiting the charge correlation of the semileptonic decay lepton (muon or electron) to the initial b charge or were using the jet charge information in selected b events. These methods suffer from the limited charge tagging efficiency, because of the relatively small semileptonic branching ratio or because of the small jet charge separation between a b quark and anti-quark jet.

This analysis improves on the charge tagging efficiency by using the full available experimental charge information from b jets. The excellent DELPHI micro vertex detector separates the particles from b hadron decays from fragmentation products on the basis of the impact parameter measurement. The hadron identification capability facilitated by the DELPHI Ring Imaging Cherenkov Counters provides a means of exploiting charge correlations of kaons or baryons in b jets. Thus, not only can the secondary b decay vertex charge be measured directly but also further information for a single jet, like the decay flavour for the different b hadron types ($\rm B^0$, $\rm B^+$, $\rm B_s$ and b baryon), can be obtained. A set of Neural Networks is used to combine the additional input with the lepton and jet charge information in an optimal way.

In order to exploit the much improved b charge tagging fully a self-calibrated method to extract the forward-backward asymmetry was developed. The b quark charge is reconstructed in both event hemispheres for a high purity sample of b events, selected using an enhanced impact parameter tag. By comparing the rate of double hemisphere tagged like-sign and unlike-sign events it is possible to extract the charge tagging efficiency directly from the data. The b quark forward-backward asymmetry is determined from the differential asymmetry of the two samples of single tagged and unlike-sign double tagged events. Here small corrections due to residual background contributions and due to charge tagging hemisphere correlations are taken into account.

The paper is organised as follows. First a short summary of the hadronic event selection is given. In section 3 the b event tagging used to obtain the high purity b quark sample is described. Section 4 details the charge tagging technique using Neural Networks

and the self-calibrating method to extract the forward backward asymmetry. Section 5 describes the measurement of A_{FB}^{b} from the DELPHI data of 1992 to 1995. Section 6 discusses the systematic errors. Finally the conclusion is given in section 7. Technical information on the self-calibration method can be found in the appendix at the end of the paper.

2 Selection of Z decays to hadrons

A detailed description of the DELPHI apparatus can be found in [4] and in the references therein. This analysis makes full use of the information provided by the tracking system, the calorimetry and the detectors for hadron and lepton identification. Of special importance is the silicon vertex detector providing three precise $R\phi$ measurements. [1] For 1994 and 1995 the extended detector accepted particles down to low θ (25°) and provided z measurements in the closest and outer shells.

This paper uses DELPHI data taken at LEP 1 from 1992 to 1995 at centre-of-mass energies in an interval of ± 0.5 GeV around the Z pole. For events entering the analysis, nominal working conditions during data taking are required at least for the central tracking detector, TPC, and for the electromagnetic calorimeters and the muon detector system. The operating conditions and efficiency of the RICH detectors varied strongly for the different data sets. These variations are included in the corresponding simulated data samples.

charged particle momentum	$\geq$	0.4 GeV/c
neutral particle energy	$\geq$	1.0 GeV
track length (tracks measured only with TPC)	$\geq$	30 cm
polar angle	$\geq$	20°
uncertainty of the momentum measured	$\leq$	100 %
impact parameter ($R\phi$)	$\leq$	4 cm
impact parameter (z)	$\leq$	10 cm

Table 1: *Cuts to select tracks.*

For each event cuts are applied to the measured particles to ensure both good quality of the reconstruction and also good agreement of data and simulation. The selections are summarised in Table 1. In addition for neutral clusters measured in the calorimeters the reconstructed shower energy had to stay above 0.3 GeV for the HPC and the STIC/SAT, and above 0.4 GeV for the EMF.

A second step selects Z decays to hadrons as explained in Table 2. Here each event is divided into two hemispheres by the plane perpendicular to the thrust axis $\vec{T}$ which is computed using the charged and neutral particles. $\theta_{\vec{T}}$ is the polar angle of the thrust axis. In addition the negligible number of events with an unphysically high momentum particle is discarded.

[1] In the DELPHI coordinate system the z-axis is the direction of the e^- beam. The radius R and the azimuth angle ϕ are defined in the plane perpendicular to z. The polar angle θ is measured with respect to the z-axis.

total energy of charged particles	$\geq$	$0.15 \times \sqrt{s}$
sum of energy of charged particles in a hemisphere	$\geq$	$0.03 \times \sqrt{s}$
total multiplicity of charged particles	$\geq$	7
multiplicity of charged particles in hemisphere	$\geq$	1
forward electromagnetic energy $E_{\mathsf{FEMC}} := \sqrt{E_{\mathsf{F}}^2 + E_{\mathsf{B}}^2}$	$\leq$	$85\% \, E_{\mathsf{beam}}$

Table 2: *Selections for Z decays to hadrons. $\sqrt{s}$ is the centre-of-mass energy.*

year	data	simulation	$\langle\sqrt{s}\rangle$
1992	636401	1727321	91.280 GeV
1993	449388	1947844	91.225 GeV
1994	1303078	3303772	91.202 GeV
1995	410629	1194970	91.288 GeV

Table 3: *Number of selected Z decays to hadrons for the different years of data taking.*

These select $2.80 \cdot 10^6$ Z decays to hadrons at a mean centre-of-mass energy of 91.234 GeV (see Table 3). The remaining backgrounds due to $\tau\tau$, Bhabha, and $\gamma\gamma$ events as well as contributions from beam-gas or beam-wall interactions are estimated to be below 0.5 % and are safely neglected in the following.

The data are compared to $8.17 \cdot 10^6$ fully simulated hadronic decays using JETSET 7.3 [5] with DELPHI tuning of fragmentation, b production and decay parameters [6].

3 Selection of Z decays to b quarks using an enhanced impact parameter method

Decays to b quarks are selected from the sample of hadronic Z decays using the DELPHI high purity b tagging. The technique is based on the well established impact parameter method used by DELPHI for the precision measurement of R_{b} [7, 8]. The analysis uses the apparent lifetime and the invariant mass of the reconstructed secondary decay as well as the energy fraction contained in the secondary vertex and the rapidities of charged particles. The latter are defined with respect to the jet direction as reconstructed with the LUCLUS algorithm [5]. The transverse momentum of the secondary vertex and identified leptons, which are supplied as additional variables for the LEP 2 enhanced b tag, are not used for this measurement.

This analysis uses a combined event tagging probability variable, $\mathrm{b_{tag}}$. Decays to b quarks tend to have higher $\mathrm{b_{tag}}$ values whereas decays to other quarks are peaked at smaller values as can be seen in Figure 1, separately for the combined years $1992 + 93$ and $1994 + 95$. High purity samples are selected by cutting on $\mathrm{b_{tag}} > 0.0$ for 1992/3 and $\mathrm{b_{tag}} > 0.4$ for 1994/5. This guarantees a constant working point over the years regardless of the change in tagging performance due to the differences in the VD set-up.

It is important to avoid a bias in the background estimates due to an imperfect description of the tagging performance in the simulation. Therefore the purities of b , c and light flavours and the efficiency for b quark events, ϵ_{b}, are corrected using the data. ϵ_{b} is

obtained from the data using:

$$\epsilon_{\rm b}(\mathrm{cut}) = \frac{\mathcal{F}(\mathrm{cut}) - R_{\rm c} \times \epsilon_{\rm c}(\mathrm{cut}) - (1 - R_{\rm c} - R_{\rm b}) \times \epsilon_{\rm uds}(\mathrm{cut})}{R_{\rm b}} \ , \tag{3}$$

where $\mathcal{F}$ is the fraction of events selected by a given cut value. $\epsilon_{\rm uds}$ and $\epsilon_{\rm c}$ are the selection efficiencies for the light flavours and the charm events, which are both obtained from the simulation. The fractions of c and b events produced in hadronic Z^0 decays, $R_{\rm c}$ and $R_{\rm b}$, are set to the LEP+SLD average values of $R_{\rm c} = 0.1731 \pm 0.0032$ and $R_{\rm b} = 0.21644 \pm 0.00068$ [10]. The corresponding purities, $p_{\rm f}$, are then calculated for each flavour using:

$$p_{\rm f}(\mathrm{cut}) = \epsilon_{\rm f}(\mathrm{cut}) \times \frac{R_{\rm f}}{\mathcal{F}(\mathrm{cut})} \ . \tag{4}$$

Accurate tuning of the simulation to the data was performed [7, 8] in order to estimate the c and light flavour background efficiencies correctly. Here each year of data taking is treated separately to allow for the changes in the detector performance. The simulated data have also been reweighted in order to represent the measured composition and lifetimes of charmed and beauty hadrons and also the rate of gluon splitting into $\mathrm{c\overline{c}}$ ($\mathrm{b\overline{b}}$) pairs correctly.

The working point at a very high b purity of $\sim 96\%$ is chosen to minimise systematic uncertainties due to background estimations. The remaining background is dominated by decays to c quarks, which is taken into account in the systematic error study.

4 The inclusive charge tagging

This section explains the novel method for inclusive b charge tagging. First the experimental information and the neural network technique used to extract the b quark flavour information from the DELPHI data are described. In the second part the self-calibrating method to extract the b quark forward-backward asymmetry is explained. This includes the technique to determine the tagging probability on data as well as a discussion of the hemisphere charge correlations and background corrections.

4.1 The Neural Network method for inclusive charge tagging

The analysis uses the full available experimental charge information from b jets which is combined into one tagging variable using a Neural Network technique. The tagging method is part of a DELPHI common analysis package for b physics called BSAURUS.In this paper only an overview of the package is given. For full details refer to reference [9].

The quark flavour tagging Neural Network is designed to distinguish between hemispheres originating from a b quark or anti-quark in $\mathrm{Z} \longrightarrow \mathrm{b\overline{b}}$ decays. The approach used is to construct a conditional probability for a given track to have the same charge as the b quark in the b hadron for both the moment of fragmentation (i.e. production) and at the moment of decay. In addition, the probabilities are constructed and processed separately for each of the b hadron types (B^0, B^+, B_s and b baryon). These probabilities are then combined with the jet charge and vertex charge information[2] in the final Neural Network.

[2]For definitions see Equations 7 and 8 below.

The first step to achieve this goal is to train a Neural Network with target output values of +1 and -1 if the charge of a particle is correlated or anti-correlated to the b quark charge. A set of predefined input variables is used to distinguish between them:

- **Selection variable for particles from secondary vertices:** A Neural Network called Tk_{net} separates particles originating from the event primary vertex from those starting at a secondary decay vertex. The separation uses the impact parameter measurement and additional kinematic information. Particles from the primary vertex lead to Tk_{net} values close to 0, while particles from a secondary vertex get values close to 1.

- **Particle identification variables:** Lepton and hadron identification information is combined into tagging variables for kaons, protons, electrons, and muons from heavy hadron decays.

- **B-D separation:** A dedicated Neural Network called BD_{net} uses decay vertex and kinematic information in a given jet to separate particles from the weak B decay from those from the subsequent cascade D decay. The target values for particles from B decay is -1, while for particles from D decay it is +1. A second variable:

$$\frac{BD_{net} - BD_{net}^{min}}{\Delta BD_{net}} \tag{5}$$

  is constructed to further isolate particles from D decays. Here again the BD_{net} is the B-D Neural Network introduced above. BD_{net}^{min} is the minimum BD_{net} value of all charged particles in the hemisphere above a Tk_{net} value of 0.5. ΔBD_{net} is the difference between the maximum and minimum value of BD_{net} for all charged particles.

- **Particle variables:** Further variables separate particles from the primary interaction from B decays. The energy of the particle and any ambiguities in reconstruction are input to the Networks. In addition, particles are boosted into the estimated B candidate rest frame. In this frame the momentum and the angle of the particle with respect to the B direction of flight are calculated.

- **Hemisphere quality variables:** For each hemisphere a set of additional variables characterise the quality of the B candidate:

  - the ratio of the reconstructed B candidate energy to the LEP beam energy,
  - invariant mass of the particles at the reconstructed B vertex,
  - the χ^2 probability of the fit for the B decay vertex,
  - the uncertainty on the vertex charge measurement,
  - the number of charged particles assigned to secondary vertices in the hemisphere with Tk_{net} above 0.5,
  - the hemisphere rapidity gap between the particles of highest rapidity below a Tk_{net} cut at 0.5 and that of smallest rapidity above the cut at 0.5; and
  - the number of particles in the hemisphere with ambiguities in reconstruction.

The networks using charged particles to distinguish the decay flavour use all input variables described above. The lepton identification and B-D separation variables do not depend on the fragmentation flavour and are therefore not used in the training of the fragmentation flavour networks.

The particle correlation conditional probabilities, $P^{time}(same\, Q_{\rm B})$, for the fragmentation and the decay flavour are then combined using a likelihood ratio to obtain a flavour tag for a given hemisphere:

$$F_{\rm B}^{time} = \sum_{particles} \ln\left(\frac{1+P^{time}(same\, Q_{\rm B})}{1-P^{time}(same\, Q_{\rm B})}\right)\cdot Q\ . \tag{6}$$

Here B is either a $\rm B^+, B^0, B_s$ or b baryon and *time* stands for *fragmentation* or *decay*. Q is the particle charge. Depending on the hypothesis considered a different selection is applied for particles entering the summation. For the fragmentation flavour all tracks with $Tk_{net} < 0.5$ are considered, while for the decay flavour a particle must satisfy $Tk_{net} \geq 0.5$.

Based on the hemisphere flavour tags defined above, the nine different inputs for the final charge tagging Neural Network are constructed. The first set of inputs is a combination of these fragmentation and decay flavour tags multiplied by the individual probabilities for that b hadron type:

(1) $F_{\rm B_s}^{Frag.}\cdot P(\rm B_s)$

(2) $\left(F_{\rm B^+}^{Dec.} - F_{\rm B^+}^{Frag.}\right)\cdot P(\rm B^+)$

(3) $\left(F_{baryon}^{Dec.} - F_{baryon}^{Frag.}\right)\cdot P(baryon)$

(4) $\left(F_{\rm B^0}^{Dec.}\cdot\left(1-2\sin^2(0.237\cdot\tau)\right) - F_{\rm B^0}^{Frag.}\right)\cdot P(\rm B^0)$

Here τ is the reconstructed proper B lifetime. The construction considers the $\rm B^0$ oscillation frequency which affects the charge information in the hemisphere. This is not possible for the case of $\rm B_s$ where the oscillations are so fast that at the time of decay a 50-50 mix of $\rm B_s$ and $\overline{\rm B}_s$ remains.

The $P(\rm B)$ factors are the outputs of a dedicated BSAURUS B species identification Network which represent probabilities that the hemisphere in question contains a weakly decaying hadron of a particular type B.

The remaining inputs are:

(5-7) The so called jet charge[3] defined as:

$$Q_J = \frac{\sum_{\rm particles} p_L^{\kappa}\cdot Q}{\sum_{\rm particles} p_L^{\kappa}}, \tag{7}$$

where the sum is over all particles in a hemisphere and p_L is the longitudinal momentum component with respect to the thrust axis. The optimal choice of the free parameter κ depends on the type of b hadron under consideration. Therefore a range of values ($\kappa = 0.3, 0.6, \infty$) are used, where the last one corresponds to taking the charge of the highest momentum particle in the hemisphere.

[3]Although the jet definitions are the hemispheres, it is called jet charge to avoid confusion with the hemisphere charge tagging network.

(8) A Vertex charge is constructed using the Tk_{net} value as a probability for each track to originate from the b hadron decay vertex. The weighted vertex charge is formed by:

$$Q_{\rm V} = \sum_{\rm particles} Tk_{net} \cdot Q \ . \tag{8}$$

(9) The significance of the vertex charge calculated using a binomial error estimator:

$$\sigma(Q_{\rm V}) = \sum_{\rm particles} \sqrt{Tk_{net} \cdot (1 - Tk_{net})} \ . \tag{9}$$

As an example the distributions of the jet charge for $\kappa = 0.3$ and 0.6 and of the vertex charge and its significance are shown in Figure 2 for data and simulation.

In addition to the flavour discriminating variables described above, use is made of 'quality' variables, e.g. the reconstructed energy of B candidate in the hemisphere. These inputs supply the network during the training process with information regarding the likely quality of the discriminating variables, and are implemented in the form of weights to the turn-on gradient (or 'temperature') of the sigmoid function used as the network node transfer function.

The training of the networks uses a standard feed-forward algorithm. The final network utilises an architecture of 9 input nodes, one for each of the variables defined above, a hidden layer containing 10 nodes and one output node. During the training, the target values at the output node for one hemisphere were -1 for a b quark or 1 for a b anti-quark.

An example of the flavour tag Neural Network output, $flav_{\rm hem}$, on the selected high purity b event sample is shown in Figure 3 for the data of 1994. The data points are compared to the simulation. The contributions from hemispheres containing b quarks and anti-quarks are shown separately for the simulation to illustrate the excellent charge separation. The difference between data and simulation in the width of the distribution indicates a small difference in the charge tagging efficiency which will be discussed in detail in the following.

In the analysis a hemisphere is flavour tagged, if the experimental information is sufficient to produce a Neural Network output $flav_{\rm hem}$ and if the absolute value $|flav_{\rm hem}|$ exceeds the work point cut of 0.35. This working point was chosen to minimise the expected relative error of the measured b asymmetry on simulated data.

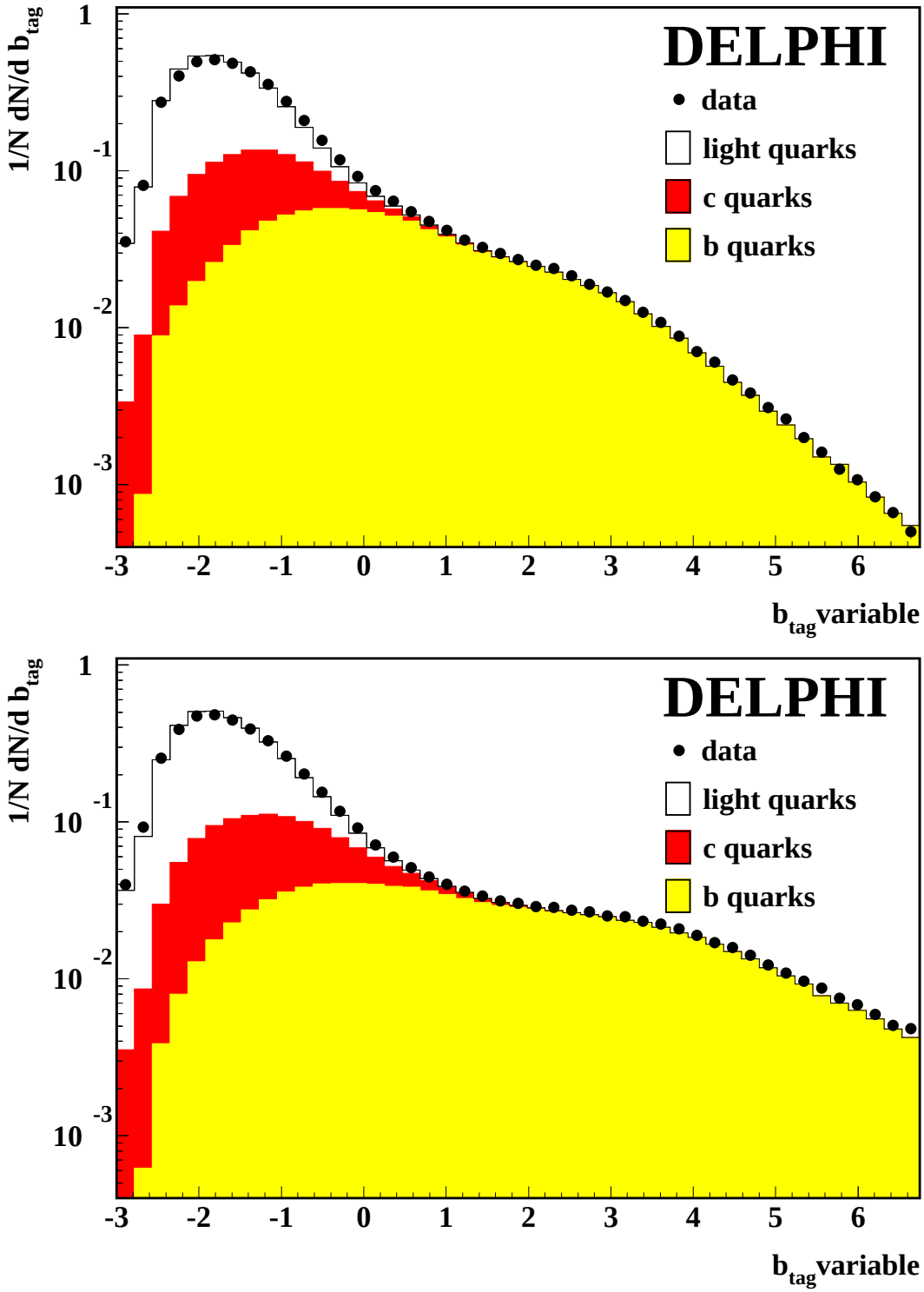

Figure 1: *Comparison between data and simulation of the normalised number of events versus the* $\mathrm{b_{tag}}$ *variable for 1992/3 (upper plot) and 1994/5 (lower plot). Light quark,* c *quark, and* b *quark events are shown separately for the simulation.*

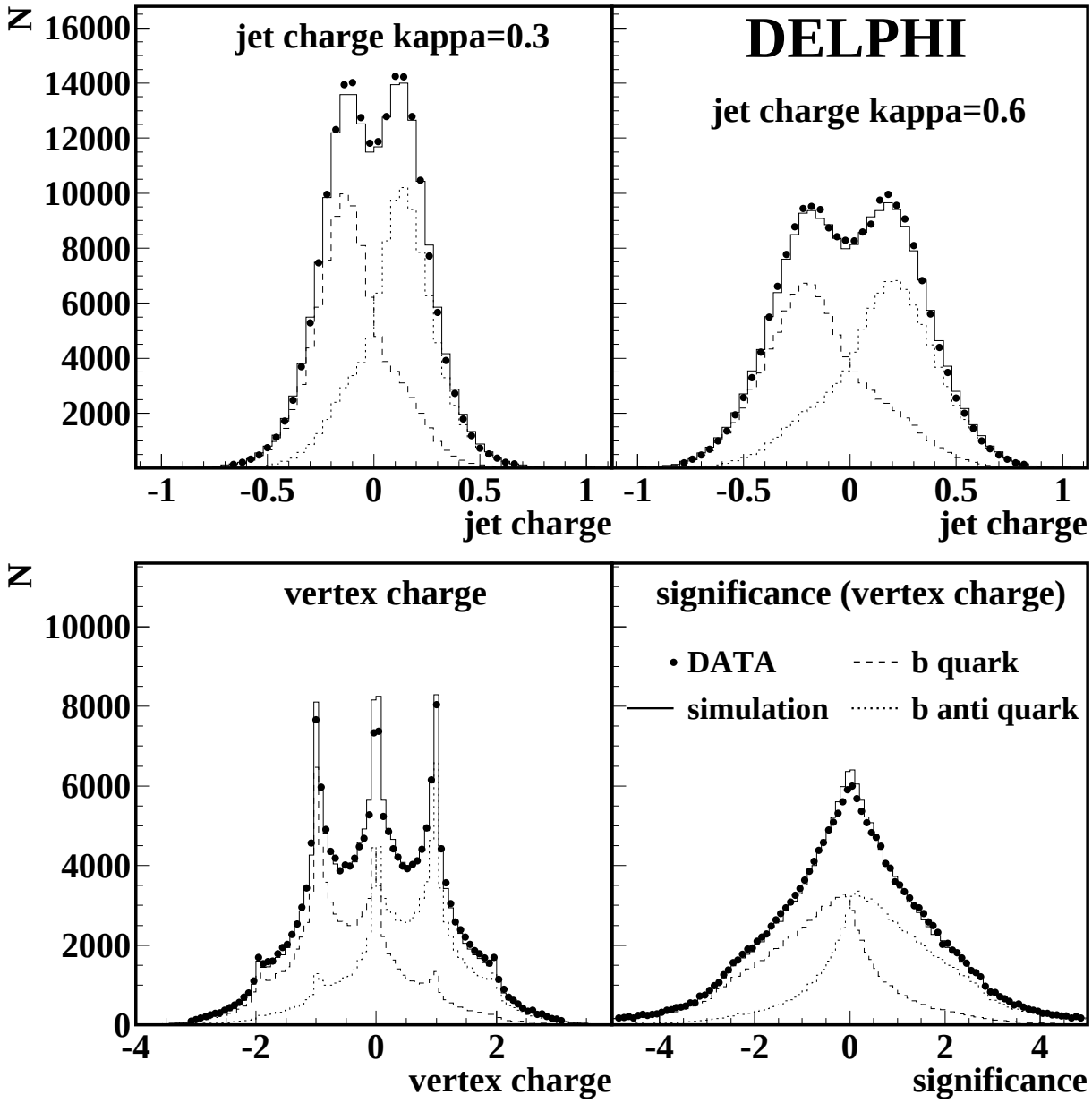

Figure 2: *The jet charge information for $\kappa = 0.3$ and 0.6 (upper plots) and the vertex charge and its significance (lower plot). Shown is the comparison between data and simulation for the data of 1994.*

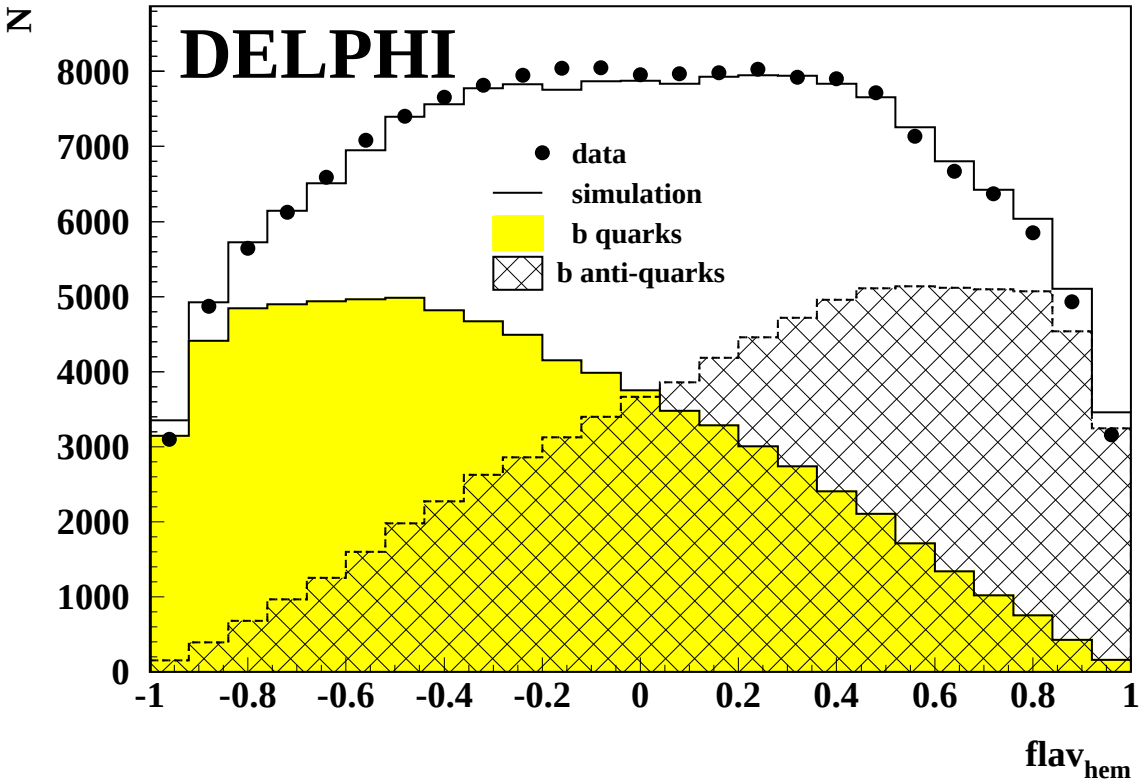

Figure 3: *Comparison between data and simulation for the flavour tag Neural Network output, $flav_{hem}$, for the data of 1994.*

4.2 Principles of the method to extract the b asymmetry

The differential cross-section for b quarks from the process $e^+e^- \to Z \to b\overline{b}$ as a function of the polar angle θ can be expressed as :

$$\frac{d\sigma}{d\cos\theta} \propto 1 + \frac{8}{3} A_{FB}^{\mathrm{b}} \cos\theta + \cos^2\theta \,. \tag{10}$$

Hence the forward-backward asymmetry generates a $\cos\theta$ dependent asymmetry in the production of b quarks. For anti-quarks the orientation (sign) of the production polar angle is reversed.

The thrust axis is used to approximate the quark direction in the analysis. The charge of the primary quark or anti-quark in a hemisphere is necessary to determine the orientation of quark polar angle $\theta_{\vec{T}}$. This charge information can be obtained separately for both event hemispheres using the flavour tag Neural Network output.

4.2.1 Single and double hemisphere tagged events

In single hemisphere tagged events the orientation of the primary quark axis is obtained from the sign of the Neural Network output. The quark axis is forward oriented ($\cos\theta_{\vec{T}} > 0$) if a forward hemisphere is tagged to contain a b quark or a backward hemisphere is tagged to contain a b anti-quark. Otherwise the quark axis is backward ($\cos\theta_{\vec{T}} < 0$) oriented.

One needs to distinguish two categories of events if both hemispheres are flavour tagged. The situation is similar to single hemisphere events when one hemisphere is tagged as quark and the other as anti-quark. Here the event orientation is determined by either hemisphere, but the additional second hemisphere flavour tag increases the probability to identify the quark charge correctly. By contrast, events for which both hemispheres are tagged to contain quarks (or both anti-quarks) do not have a preferred orientation. These like-sign events are used to measure the charge tagging probability.

4.2.2 The observed asymmetry

The difference of the number of forward and backward events normalised to the sum is the forward-backward asymmetry. Thus for single hemisphere tag events:

$$A_{FB}^{obs} = \frac{N - \overline{N}}{N + \overline{N}} = \sum_{\mathrm{f=d,u,s,c,b}} (2 \cdot w_{\mathrm{f}} - 1) \cdot A_{FB}^{\mathrm{f}} \cdot p_{\mathrm{f}} \cdot \eta_{\mathrm{f}} \ , \tag{11}$$

where

$$\begin{array}{rcl} N & = & \text{number of single hemisphere tagged forward events,} \\ \overline{N} & = & \text{number of single hemisphere tagged backward events.} \end{array}$$

Similarly for the double hemisphere tagged events:

$$A_{FB}^{D,obs} = \frac{N^D - \overline{N^D}}{N^D + \overline{N^D}} = \sum_{\mathrm{f=d,u,s,c,b}} (2 \cdot w_{\mathrm{f}}^D - 1) \cdot A_{FB}^{\mathrm{f}} \cdot p_{\mathrm{f}}^D \cdot \eta_{\mathrm{f}} \ , \tag{12}$$

where

N^D = number of double hemisphere tagged forward events,
$\overline{N^D}$ = number of double hemisphere tagged backward events.

The observed asymmetry is the sum of the contributions from b events and from c and uds background events. A_{FB}^{f} is the forward-backward asymmetry, p_{f} and p_{f}^D are the purities for each flavour in the single and double tagged events categories. The η-term accounts for the differently signed charge asymmetries, $\eta_{\mathrm{f}} = -1$ for up-type quarks and $\eta_{\mathrm{f}} = 1$ for down-type quarks.

w_{f} and w_{f}^D are the probabilities to identify the quark charge correctly in single and double tagged events. For single tagged events:

$$w_{\mathrm{f}} = \frac{\hat{N}_{\mathrm{f}} + \hat{N}_{\overline{\mathrm{f}}}}{N_{\mathrm{f}} + N_{\overline{\mathrm{f}}}} \quad , \tag{13}$$

where $N_{\mathrm{f}}(N_{\overline{\mathrm{f}}})$ is the number of simulated events, which contain a quark (anti-quark) in the forward hemisphere. $\hat{N}_{\mathrm{f}}(\hat{N}_{\overline{\mathrm{f}}})$ is the number of events, in which the quark (anti-quark) has been correctly identified.

For unlike-sign events the fraction of events, in which both quark and anti-quark charges are correctly identified, is defined analogously to the single hemisphere tagged events as the ratio of correctly tagged $(\hat{N}_{\mathrm{f}}^D, \hat{N}_{\overline{\mathrm{f}}}^D)$ over all double-tagged unlike-sign $(N_{\mathrm{f}}^D, N_{\overline{\mathrm{f}}}^D)$ events:

$$w_{\mathrm{f}}^D = \frac{\hat{N}_{\mathrm{f}}^D + \hat{N}_{\overline{\mathrm{f}}}^D}{N_{\mathrm{f}}^D + N_{\overline{\mathrm{f}}}^D} \quad . \tag{14}$$

To measure the b quark forward-backward asymmetry all quantities appearing in Equations 11 and 12 have to be determined. The rates N, $\overline{N}$, N^D, $\overline{N^D}$ are obtained from the data. The b purity, p_{b}, and the probability to correctly identify the b quark charge can also be extracted directly from data with only minimal input from simulation. The determination of p_{b} was discussed in section 3, the measurement of w_{b} and w_{b}^D are discussed in the next section. Small corrections due to c and light quark backgrounds and to hemisphere correlations (see Section 4.4) are based on simulation.

4.3 The probabilities to identify the b quark charge correctly

For the case of b quarks the probabilities to identify the charge correctly can be measured directly from the data leading to a self-calibration of the analysis. The principle idea of the method is that the unlike-sign and like-sign double tagged events are proportional to:

$$N^D + \overline{N^D} \propto [w_{\mathrm{b}}^2 + (1 - w_{\mathrm{b}})^2] \; , \tag{15}$$

$$N^{same} \propto 2 \cdot w_{\mathrm{b}} \cdot (1 - w_{\mathrm{b}}) \; . \tag{16}$$

where

N^{same} = number of double tagged like-sign events.

Resolving the quadratic equations leads to:

$$w_{\mathrm{b}} \cdot \sqrt{1+\delta} = \frac{1}{2} + \sqrt{\frac{1}{4} - \frac{1}{2} \cdot \frac{N^{same} \cdot p_{\mathrm{b}}^{same}}{[N^D + \overline{N^D}] \cdot p_{\mathrm{b}}^D + N^{same} \cdot p_{\mathrm{b}}^{same}}} \; , \tag{17}$$

$$w_{\mathrm{b}}^{D} \cdot \sqrt{1+\beta} = \frac{{w_{\mathrm{b}}}^2 \cdot (1+\delta)}{{w_{\mathrm{b}}}^2 \cdot (1+\delta) + (1 - w_{\mathrm{b}} \cdot \sqrt{1+\delta})^2} \ . \tag{18}$$

A detailed derivation of these equations can be found in the appendix. p_{b}^{D} and p_{b}^{same} are the b purities determined individually for the unlike-sign and like-sign categories using equations 3 and 4. The additional terms $\sqrt{1+\delta}$ and $\sqrt{1+\beta}$ allow for hemisphere charge correlations and are discussed in section 4.4.

In Figure 4 the measured probabilities for single and double tagged events are shown as a function of the polar angle for the year 1994. The results on data are corrected for tiny background contributions and are compared to the prediction from simulation. In double tagged events w_{b}^{D} is found to be above 92 % and drops to 85 % for large $\cos\theta_{\vec{T}}$ near the edge of the detector acceptance. A similar behaviour is found for the single tagged events.

4.4 The correlations δ and β

The probabilities to identify the quark charge correctly are deduced from double hemisphere tagged like-sign and unlike-sign events. Correlations between the two hemisphere charge tags in different event categories affect the measurement and need to be taken into account. The term $\sqrt{1+\delta}$ in Equation 17 allows for such correlations when calculating the single tagged probability, w_{b}, using the double tagged events. The probability to identify the quark charge in double tagged unlike-sign events, w_{b}^{D}, is obtained from w_{b} using Equation 18. Here the additional term $\sqrt{1+\beta}$ allows for the different correlations in double tagged unlike-sign events.

The correlation terms $\sqrt{1+\delta}$ and $\sqrt{1+\beta}$ are obtained from simulation using b quark events. The result of the right hand side of Equation 17 can be compared to the true tagging probability for single tagged events calculated using the simulation truth. The ratio of both results is given by the term $\sqrt{1+\delta}$. Similarly the term $\sqrt{1+\beta}$ is deduced from the ratio of the result from the right hand side of Equation 18 and the truth in double tagged unlike-sign events. In Figure 5 the correlations δ (upper plot) and β (lower plot) are shown as a function of the polar angle $\cos\theta_{\vec{T}}$ for the different years of data taking. Within errors the correlations are stable as a function of the polar angle up to the end of the acceptance.

Possible sources of the hemisphere charge correlation have been investigated in detail. In order to understand the origin of the correlations, experimental input variables were consecutively discarded from the charge tagging Neural Network. With the charge tagging modified in this way, the measurement was repeated. Only for the charge network for which the jet charges for $\kappa = 0.3$ and $\kappa = 0.6$ were omitted was a significant variation in the correlation observed. The mean of the correlations $\langle\delta\rangle$ and $\langle\beta\rangle$ calculated with this flavour tag are shown as dashed lines in Figure 6. This can be compared to the dependence of the correlation for the full Neural Network as a function of the cut on the flavour tag output $|flav_{\mathrm{hem}}|$, which is shown as points. Almost no correlation for $\langle\delta\rangle$ and only a small correlation for $\langle\beta\rangle$ remain after removing the jet charge information.

The source of hemisphere charge correlations for the jet charge analysis has been studied in reference [2]. It was found that the dominant sources of correlations are charge conservation in the event and QCD effects introduced by gluon radiation. The charge conservation effect is found to be most pronounced for $\kappa = 0.3$, which gives highest weights to soft tracks. The same behaviour is found for the flavour tagging Neural Network when

removing the jet charge from the network input. The hemisphere charge correlations δ and β are also sensitive to gluon radiation. This behaviour is illustrated in Figure 6 by applying a cut on the thrust value of $|\vec{T}| > 0.9$ to the events before entering both versions of the Network.

Further possible sources of correlations have been investigated. The beam spot is shifted with respect to the centre of the DELPHI detector. Furthermore its dimension differs in x and y by more than one order of magnitude. A possible ϕ structure in the mean correlations $\langle\delta\rangle$ and $\langle\beta\rangle$ has been investigated by comparing results for different intervals of the thrust azimuthal angle, $\phi_{\vec{T}}$. No significant variation has been found.

5 The measurement of A_{FB}^{b}

The differential asymmetry is insensitive to changes in the detector efficiency between different bins in polar angle. Hence the measurement of the b asymmetry is done in consecutive intervals of $\cos\theta_{\vec{T}}$. According to the different VD set-ups, eight equidistant bins covering $\cos\theta_{\vec{T}} \in [0.0, 0.8]$ are chosen for 1992 and 1993, and nine bins covering $\cos\theta_{\vec{T}} \in [0.0, 0.9]$ for 1994 and 1995. In each bin the observed asymmetry is given by replacing the b quark forward-backward asymmetry A_{FB}^{b} in Equations 11 and 12 by the differential asymmetry:

$$A_{FB}^{\mathrm{b,diff}}(\cos\theta_{\vec{T}}) \;=\; \frac{8}{3}\cdot A_{FB}^{\mathrm{b}}\cdot\frac{\cos\theta}{1+\cos^2\theta}\;. \tag{19}$$

To extract A_{FB}^{b} all parameters of Equations 11 and 12 need to be determined bin by bin. The probabilities w_{b} and w_{b}^D to identify the b quark charge correctly as a function of the polar angle were discussed above. This includes corrections for the hemisphere correlations for each bin.

After the complete selection, the combined data sample of single and unlike-sign double flavour tagged events contains a b fraction p_{b} of close to 96 %. In Figure 7 the $\cos\theta_{\vec{T}}$ dependence of the b purities p_{b} and p_{b}^D and of the b efficiencies ϵ_{b} and ϵ_{b}^D is shown. The data is compared to the simulation. Both efficiency and purity are stable in the central region of the detector. At large $\cos\theta_{\vec{T}}$ the purity increases slowly for both categories of single and double tagged events. At the same time the b efficiency decreases with a fast drop for $\cos\theta_{\vec{T}} > 0.7$. This effect is due to a decreasing detector performance for the b tagging causing only events with a clear b signature to be tagged. The simulation reproduces the shape of the data.

Small corrections for c and light quark backgrounds in Equations 11 and 12 are estimated from simulation. For all non-b flavours the probability of identifying the quark charge correctly is calculated in each bin from the simulation using Equation 13 for the single tagged and Equation 14 for the double tagged events. The corresponding purities are estimated based on the efficiencies from simulation using Equation 4.

The background forward-backward asymmetries for d, u and s quark events are set to the Standard Model values, and for c events the forward-backward asymmetry is set to its measured LEP value ($A_{FB}^{\mathrm{c}} = 0.0689 \pm 0.0035$) [10].

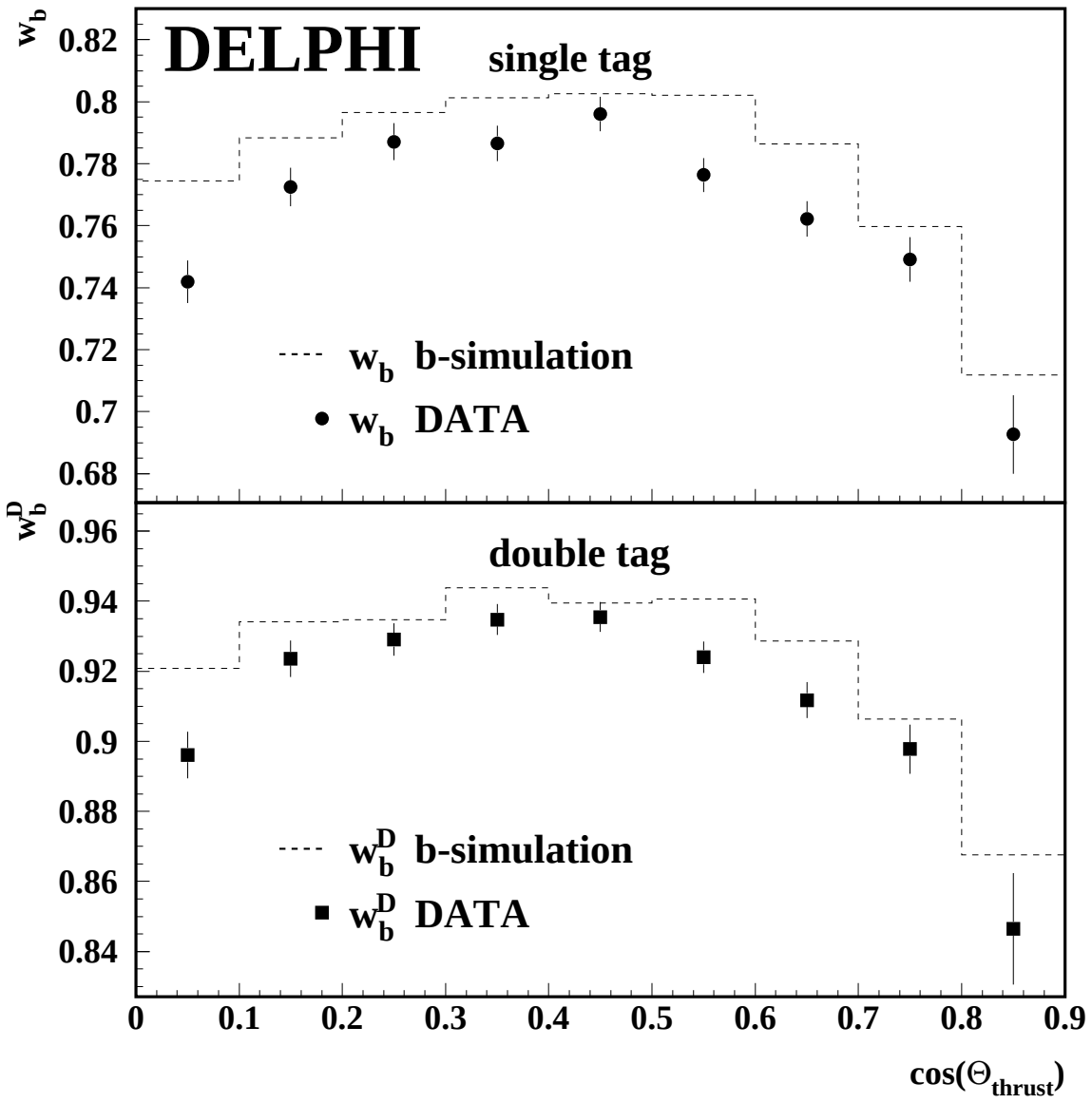

Figure 4: *The probability to identify b quarks correctly for data and simulation for the year 1994. The upper plot shows the result for single tagged events, the lower for double tagged events. See text for details.*

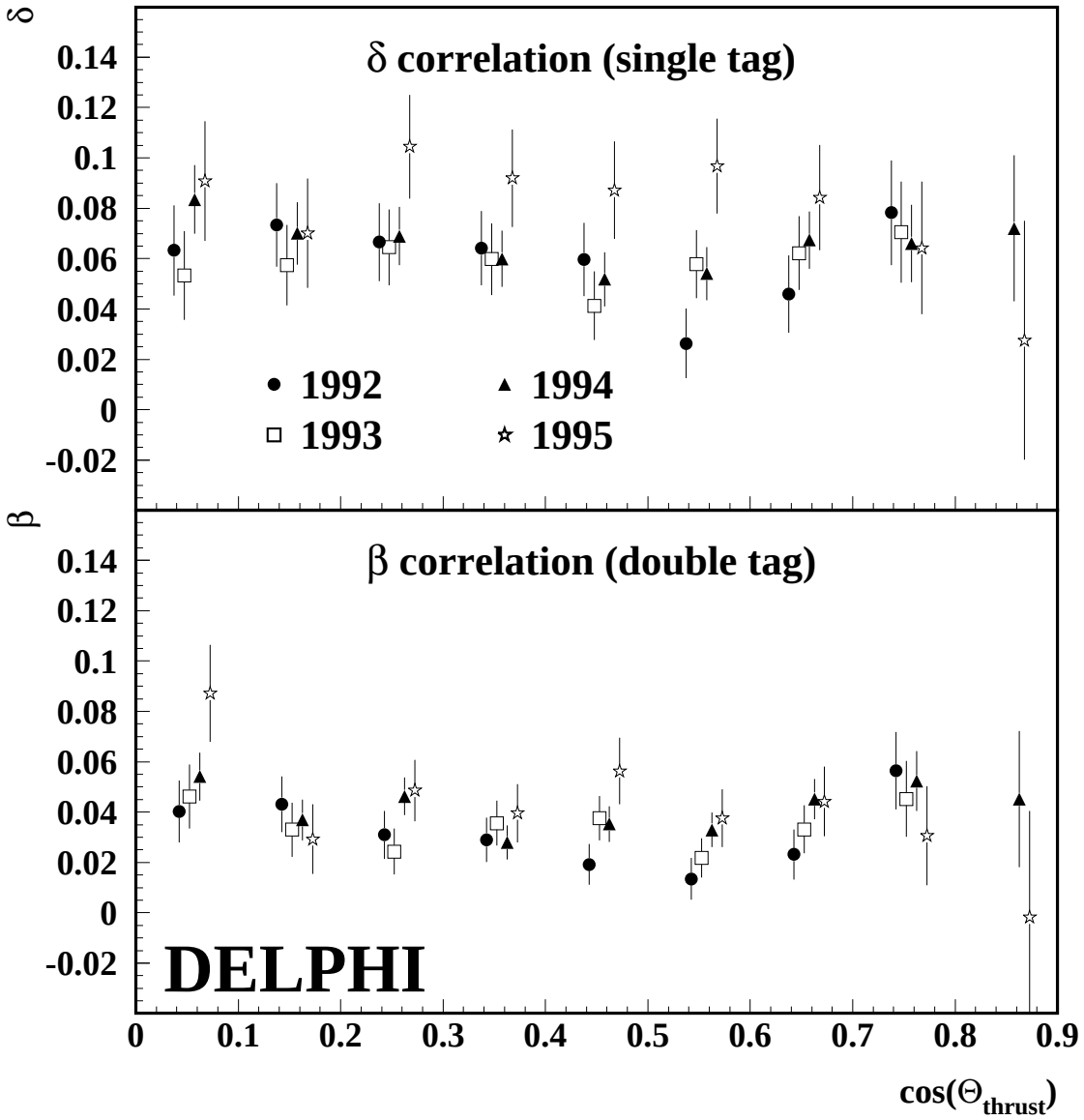

Figure 5: *Correlation of single and double tagged events simulated for the years 1992 to 1995.*

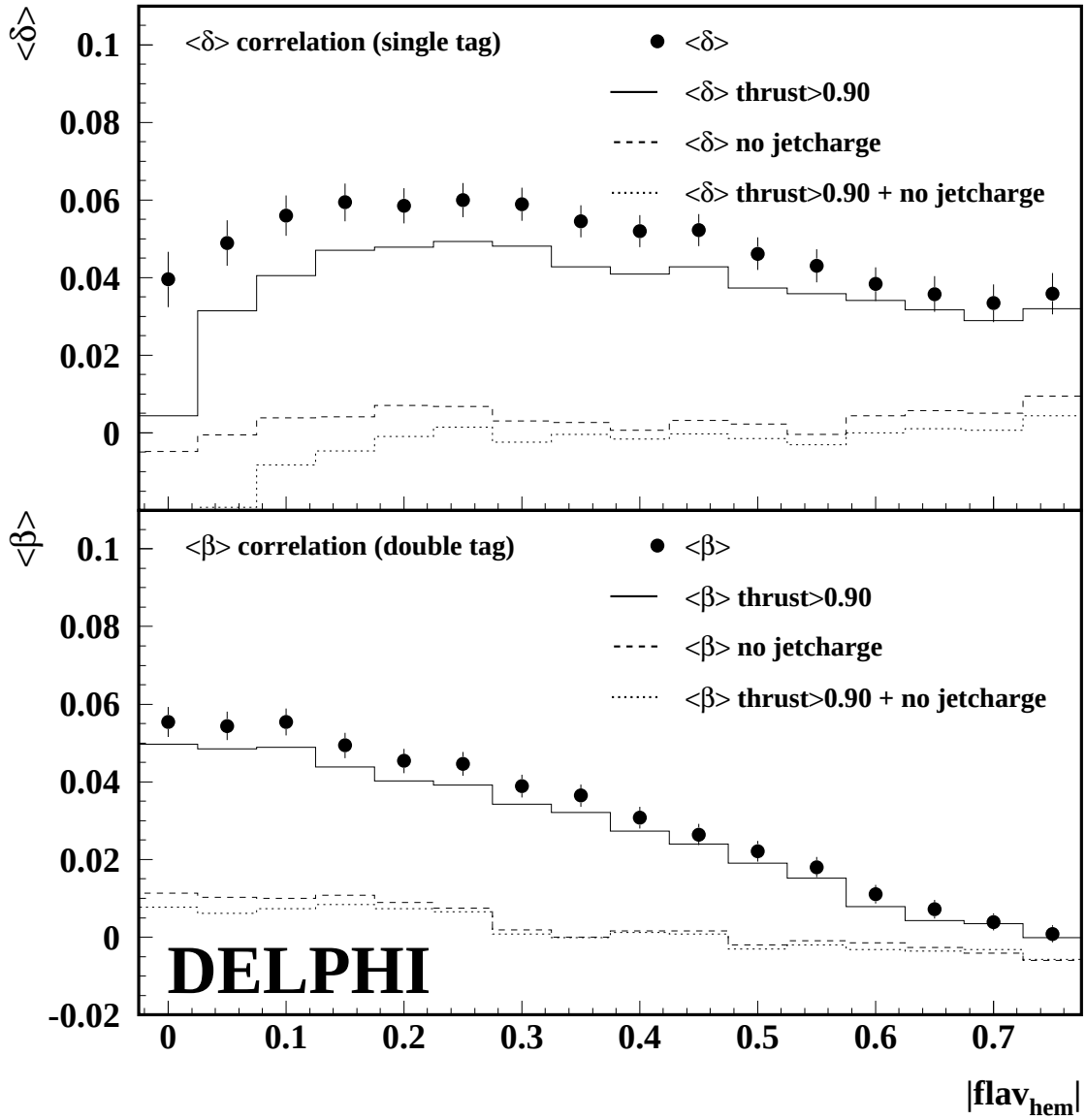

Figure 6: *The mean of the correlations δ and β of 1994 simulation as a function of the cut on the flavour tag output $|flav_{hem}|$. Besides the full flavour network (points) results using modified flavour networks without the jet charge input and both with an additional cut on the thrust value, $|\vec{T}| > 0.9$, are shown. Statistical uncertainties of the lines are slightly increased with respect to the points.*

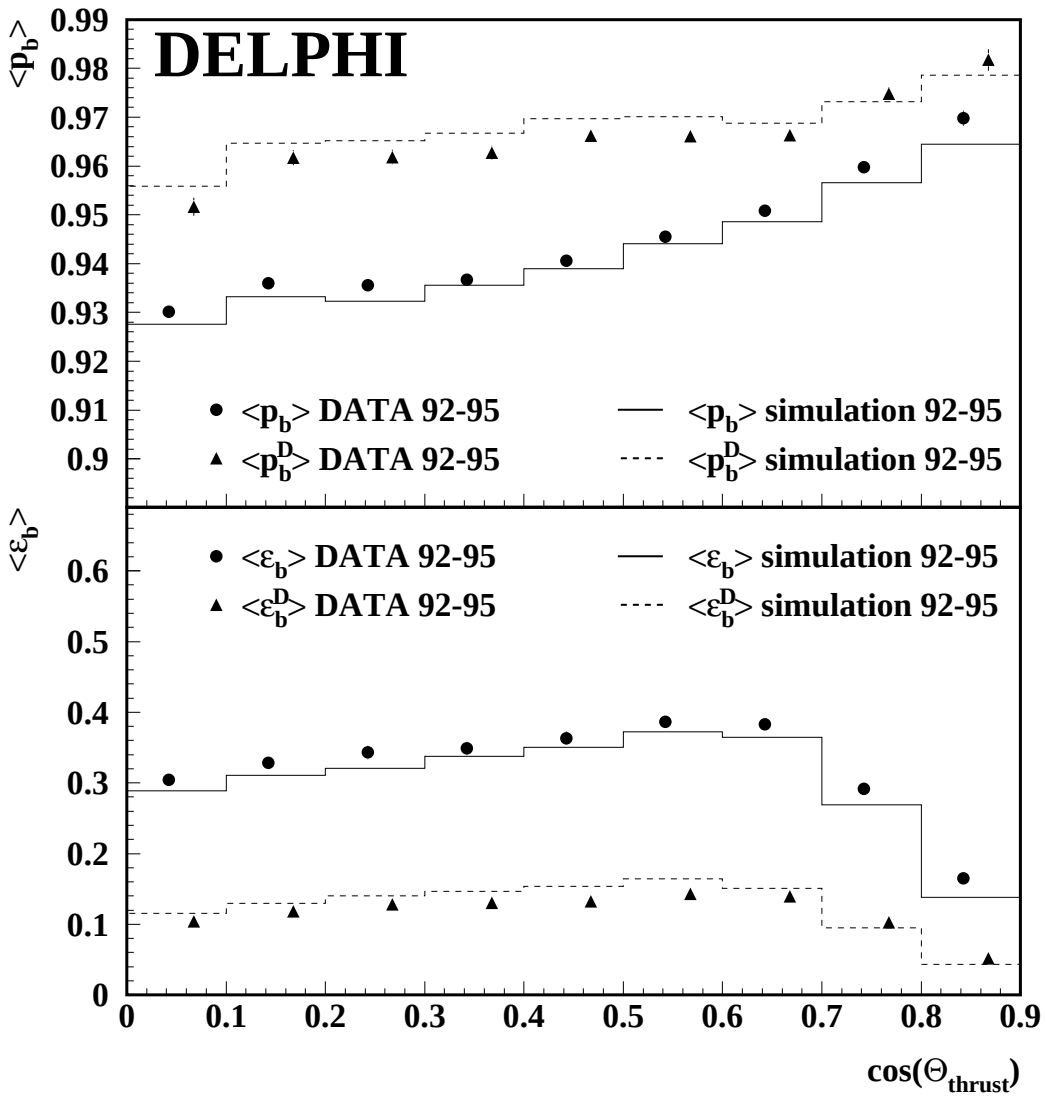

Figure 7: *The b purities* p_{b} *and* p_{b}^{D} *and the efficiencies* ϵ_{b} *and* $\epsilon_{\mathrm{b}}^{D}$ *for single and double tagged events as a function of the polar angle.*

5.1 The QCD correction

The measurement of the b quark forward-backward asymmetry is sensitive to QCD corrections to the quark final state. These corrections are known up to the 2nd order for massless quarks for a measurement using the thrust axis to approximate the initial quark direction.

A realistic measurement has a reduced experimental sensitivity to the QCD effects because of biases in the analysis against events with hard gluon radiation. In this analysis the flavour tagging and also the b tagging introduce a bias against QCD effects. Therefore the QCD correction can be written as [11]:

$$A_{FB}^{\mathrm{b},QCD} = (1 - C_{\mathrm{b}}) A_{FB}^{\mathrm{b},noQCD} = (1 - s_{\mathrm{b}}\, C_{QCD}^{\mathrm{b}}) A_{FB}^{\mathrm{b},noQCD}. \tag{20}$$

Here $A_{FB}^{\mathrm{b},noQCD}$ is the asymmetry of the initial b quarks without gluon radiation, which can be calculated from the measured asymmetry $A_{FB}^{\mathrm{b},QCD}$ through the correction coefficient C_{b}. This correction coefficient can be decomposed into a product of the full QCD correction C_{QCD}^{b} to the b quark asymmetry measured using the thrust direction and the sensitivity s_{b} of the individual analysis to C_{QCD}^{b}. By this means the QCD correction on simulated data, where its value [11] is subject to physics and detector modelling, is permitted to be different from the correction foreseen for real data. The latter has been newly estimated in reference [12], giving

$$C_{QCD}^{\mathrm{b,\,sim.}} = (3.06 \pm 0.03)\% \qquad \text{and} \qquad C_{QCD}^{\mathrm{b,\,est.}} = (3.54 \pm 0.63)\% \quad . \tag{21}$$

The experimental bias is studied on simulation by fitting the differential asymmetry of the b simulation after setting the generated asymmetry of the initial b quarks before gluon radiation to the maximum of 75%. The observed relative differences of the asymmetries are studied separately for each $\cos\theta_{\vec{T}}$ interval. In Figure 8 the coefficient C_{b} is shown for single and double tagged events for the different years. At small polar angles the sensitivity to the asymmetry is small and hence C_{b} receives a larger statistical uncertainty. No clear systematic variation is seen at large polar angles.

year	s_{b} [%]
1992	22 ± 8
1993	22 ± 8
1994	12 ± 5
1995	20 ± 9

Table 4: Summary of bias factors s_{b} with their statistical uncertainty.

From the coefficient C_{b} the experimental bias factor s_{b} is deduced. The averaged values of s_{b} are shown in Table 4 for the different years of data taking. In the following the correction coefficients $s_{\mathrm{b}} \cdot C_{QCD}^{\mathrm{b,\,est.}}$ are taken into account for each bin in polar angle separately and hence all asymmetries quoted are corrected for QCD effects.

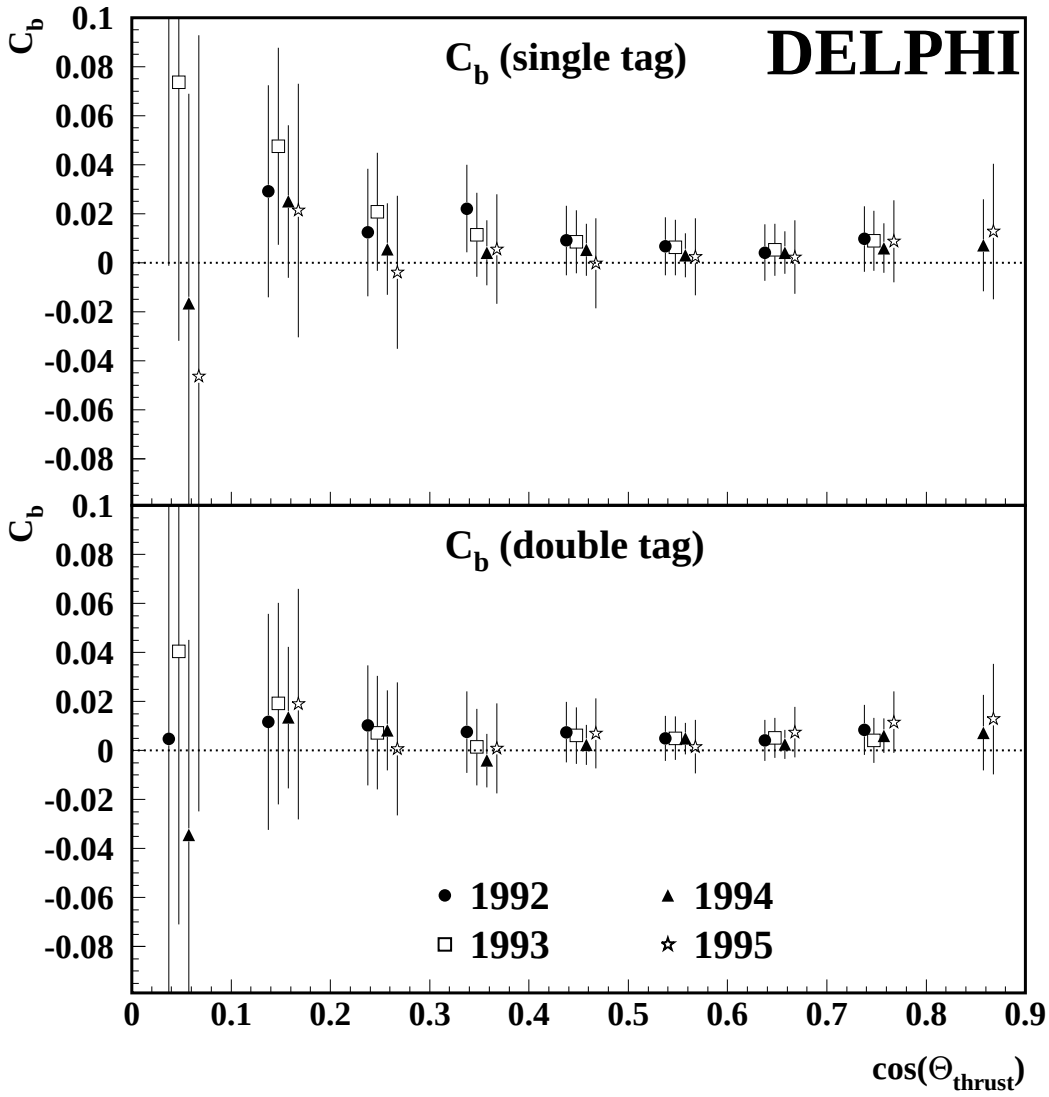

Figure 8: *The size of the QCD correction including experimental biases as a function of the polar angle of the thrust axis. In the upper plot the correction is shown for single tagged events from the different years. In the lower plot the corresponding corrections are shown for double tagged events. The statistical errors on the points are overestimated neglecting the influence of some correlations in the error propagation.*

5.2 The fit of the b quark forward-backward asymmetry

The b quark forward-backward asymmetry is extracted from a χ^2-fit dividing the data of each year in 4 intervals of b_{tag}. This allows for the change in b-purity and in the size of the hemisphere correlations as a function of b_{tag}. Technically A_{FB}^{b} is extracted in each interval from a χ^2-fit to the five independent event categories N, $\overline{N}$, N^D, $\overline{N^D}$and N^{same} in bins of polar angle.

The double hemisphere tagged unlike-sign events are sensitive to the asymmetry, but the rates also enter into the determination of the charge tagging probabilities w_{b} and w_{b}^D, as can be seen in Equations 17 and 18. This leads to correlations between the probabilities and the measured asymmetry in each bin. In the combined χ^2-fit to the five event rates N, $\overline{N}$, N^D, $\overline{N^D}$ and N^{same} these correlations are taken into account. Using the equations above, the rates can be expressed as a function of the b quark forward-backward asymmetry A_{FB}^{b}, the probability w_{b} and two arbitrary normalisation factors which absorb the overall efficiency corrections. These normalisations are set to their proper values for each bin in the fit. It has been cross-checked on simulation that the fitted forward-backward asymmetry A_{FB}^{b} results in the true forward-backward asymmetry A_{FB}^{b} of the b quarks.

In figure 9 the measured asymmetries with their statistical errors are shown in intervals of b_{tag} for the different years. The band represents the overall result. Figure 10 shows the measured differential asymmetry for single and double tagged events as a function of $\cos\theta_{\vec{T}}$ averaged over all years of data taking and over all b_{tag} intervals. Again, only statistical errors are shown and the band represents the overall result.

year	$\sqrt{s}$ [GeV]	A_{FB}^{b}
1992	91.280	0.1008 ± 0.0082
1993	91.225	0.1027 ± 0.0099
1994	91.202	0.0959 ± 0.0049
1995	91.288	0.0910 ± 0.0087

Table 5: Summary of the A_{FB}^{b} results for the different years with their statistical error.

The summary of the individual A_{FB}^{b} results for the different years with their statistical uncertainties is given in Table 5. Combining these measurements taking common uncertainties into account yields the final result:

$$A_{FB}^{\mathrm{b}}(91.234\ \mathrm{GeV}) \quad = \quad 0.0967 \pm 0.0036(\mathrm{stat.}) \quad .$$

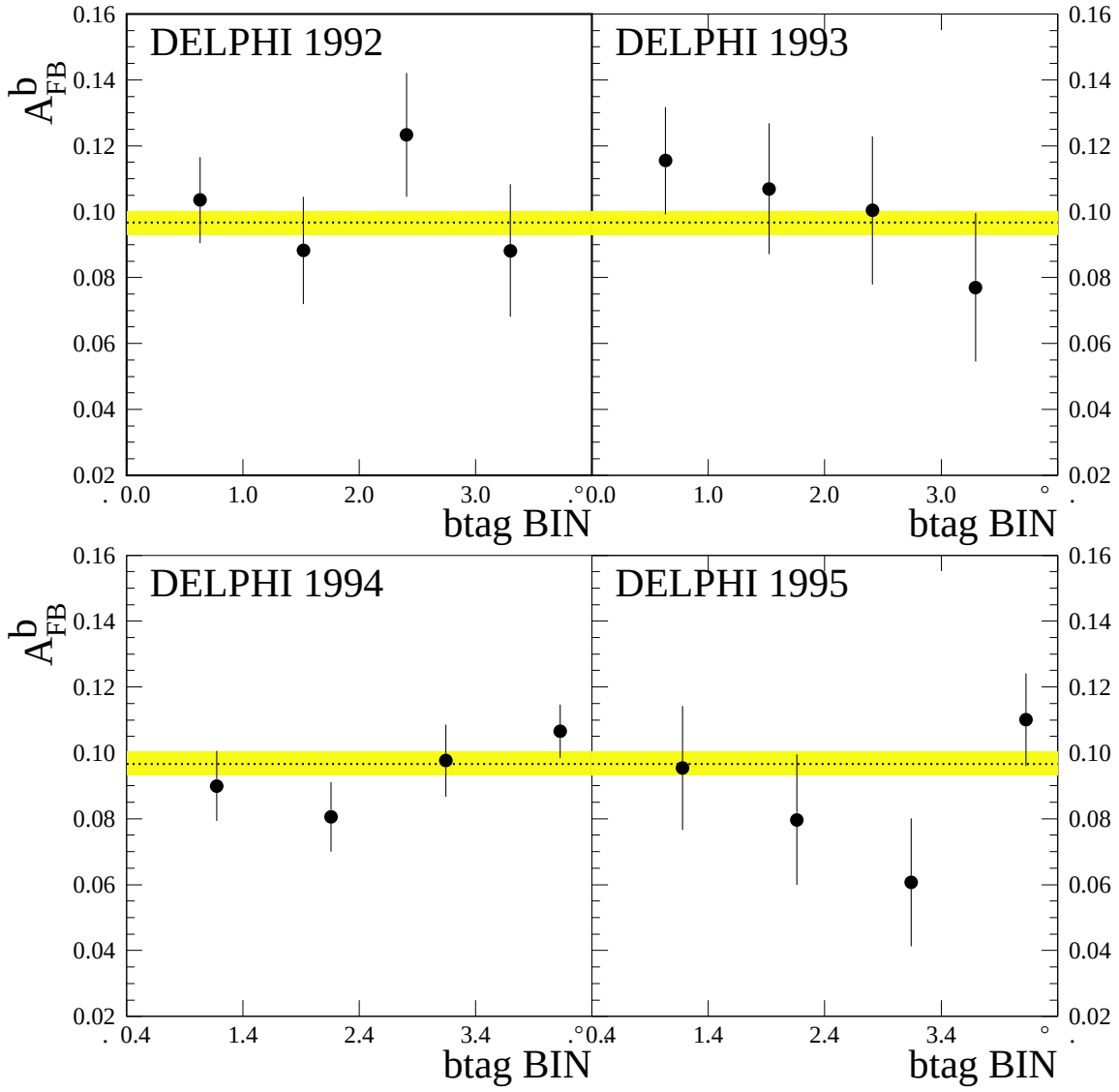

Figure 9: *The A_{FB}^{b} results for each year and each interval in b_{tag} with their statistical errors. The 16 individual measurements enter into the final fit taking into account statistical and systematic errors. The line is the result of the χ^2-fit with its statistical error shown as the band.*

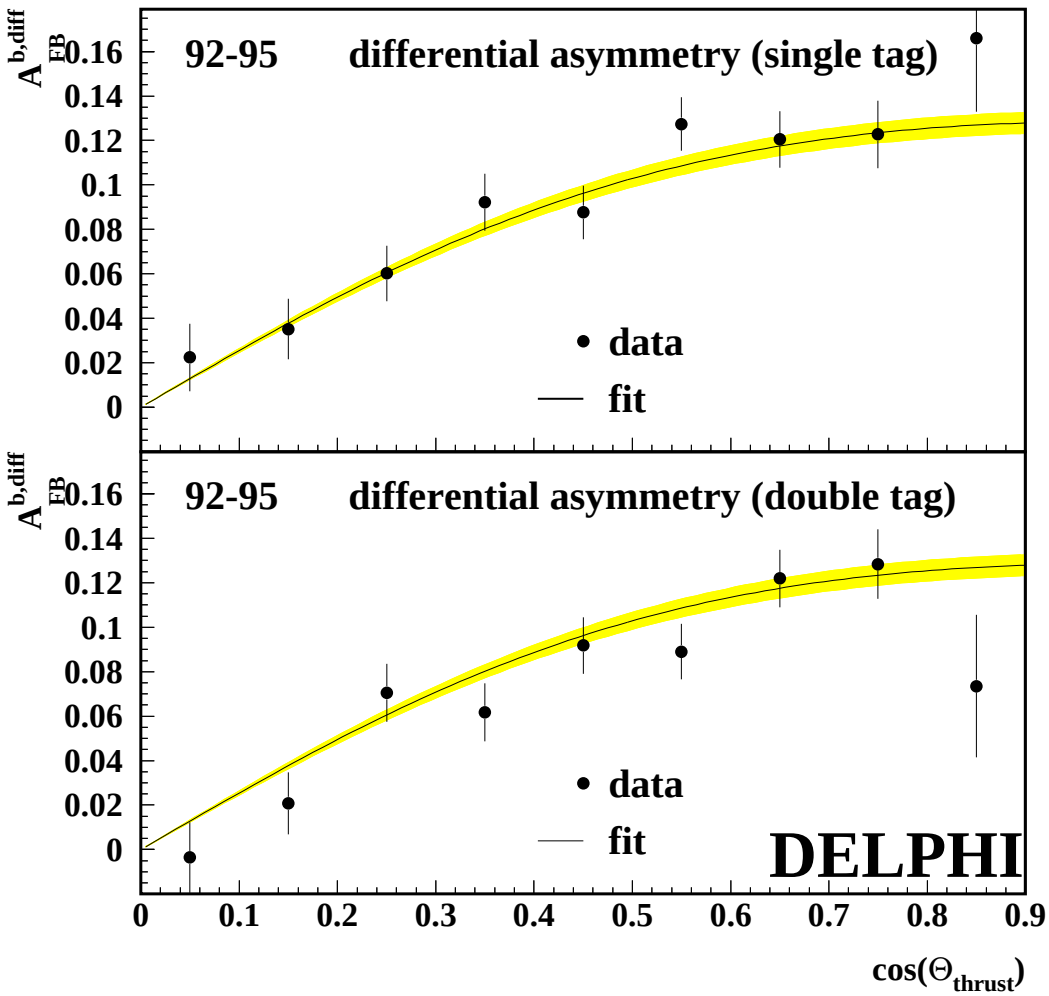

Figure 10: *The differential b quark forward-backward asymmetry of the years 1992 to 1995. The line is the result of the χ^2-fit with its statistical error shown as the band.*

6 Discussion of systematic uncertainties

The two main components of the analysis are the enhanced impact parameter b tagging and the Neural Network charge tagging. Both components are sensitive to detector resolution effects as well as to the modelling of light and charm quark events in the simulation. Therefore variations of these quantities are studied and changes in the result are propagated through the whole analysis chain. The variation of systematic errors as a function of the b_{tag} intervals is taken into account.

The systematic error sources affecting the measurement are:

- In the measurement the LEP+SLD average values [10] for the electroweak parameters $R_{\mathrm{b}} = 0.21644 \pm 0.00068$, $R_{\mathrm{c}} = 0.1731 \pm 0.0032$ and $A_{FB}^{\mathrm{c}} = 0.0689 \pm 0.0035$ are used. These parameters are used to determine the purities of the different flavours in the selected data sets and to subtract the background asymmetry in the measurement. Variations of $\pm 1\sigma$ with respect to the LEP+SLD averages are included in the systematic error.

- The detector resolution on the measured impact parameter affects both, the b tagging and the charge tagging in a similar fashion, because both tagging packages exploit the lifetime information in the events. A bad description of the resolution in the simulation may lead to a wrong estimation of remaining background in the sample. In the analysis a careful year by year tuning of these resolutions and of the vertex detector efficiency has been used [7] for both tagging packages.

  For the systematic error estimation the recipe from the DELPHI R_b measurement [8] was followed. First the calibration of the impact parameter significance for the simulation was replaced by the corresponding one for the real data to test residual differences between data and simulation. Second the VD efficiency correction was removed from the simulation. Finally the resolution of the impact parameter distribution was changed by $\pm 1\sigma$ with respect to the measured resolution in a real data sample depleted in b events. The systematic uncertainty quoted was chosen conservatively as the linear sum of all three contributions, for which the last one gives the dominant uncertainty.

- For the charge tagging Neural Networks a hemisphere 'quality' information is used to determine the likely quality of the discriminating variables. This information includes the number of good tracks reconstructed in the VD in a hemisphere and the number of ambiguities found in the track reconstruction. After the impact parameter tuning described above an additional year by year correction has been applied to the simulation to allow for remaining small differences in the hemisphere 'quality' information w.r.t. the data. 50 % of the effect of this correction is quoted as a systematic error.

- The b quark charge identification probability is measured directly from data using the double tagging technique described above. Small correlations between the charge identification probability in each $\cos\theta_{\vec{T}}$ bin and A_{FB}^{b} via the double tagged opposite sign events are therefore automatically taken into account. The statistical uncertainties of the charge identification probabilities w_{b} and w_{b}^{D} are determined in the χ^2-fit and are included in the statistical error on A_{FB}^{b}.

- The charge separation for the background of charm events determines directly the background asymmetry correction. Because the measured c asymmetry enters in the measurement with the opposite sign w.r.t. the b asymmetry, it is a potentially important source of systematic error. Therefore the charge identification probability has been measured directly from data using a set of exclusively reconstructed D meson events. Figure 11 shows the product of the hemisphere charge tag multiplied with the sign of the D^* from fully reconstructed $D^{*+} \to (K^+\pi^-)\pi^-$ decays. For these hemispheres the D^* determines the charge of the c quark or of the b quark at the time of the decay. A strong correlation between both charges is observed which illustrates the charge tagging power exploited in this measurement.

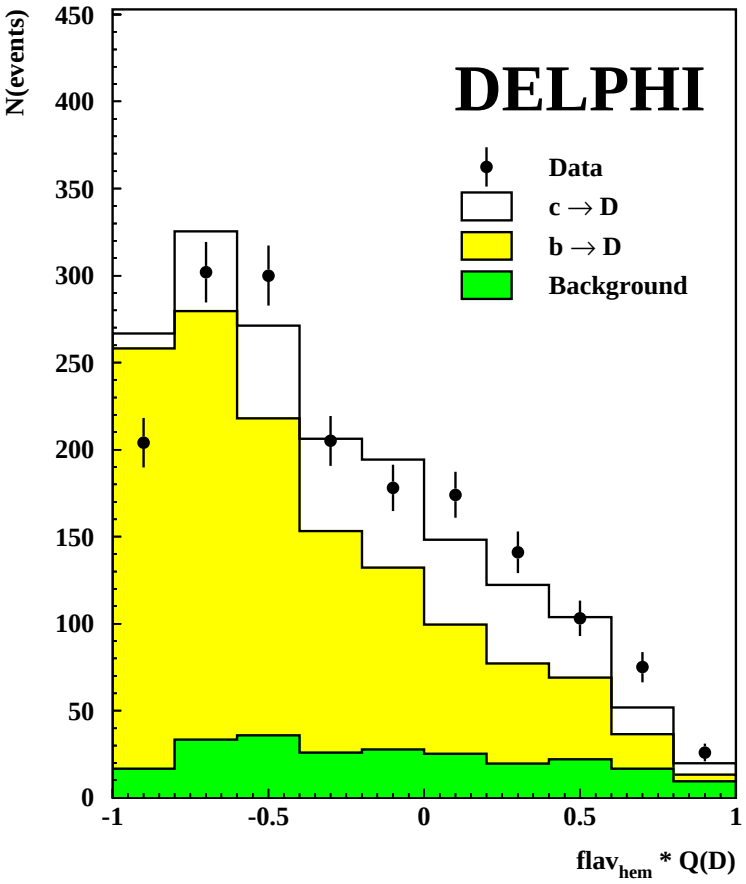

Figure 11: *The product of the charge tagging Neural Net output times the charge of a reconstructed* $D^{*+} \to (K^-\pi^+)\pi^+$ *in the same hemisphere. The data is compared to the simulation, which is split into b , c and background events.*

The charm charge tagging probability of the Neural Net was determined using the $flav_{\rm hem}$output from hemispheres opposite to a reconstructed D meson. This analysis is based on the full data set of 9 different exclusive D decay modes used by DELPHI to measure the charm asymmetry [13]. The same cuts used in the rest of this paper were applied to this sample. To separate the contributions from c and b events a two dimensional fit was performed using the D energy and the b tagging information in the D hemisphere as separating variables. The latter allows for the correlation between the hemisphere b-tag and the hemisphere charge tagging. To avoid biases,

corrections for $B-\bar{B}$ mixing and for upper vertex charm were taken into account for the D hemispheres. Combining all decay modes a relative difference in the charm charge tagging probability of $-4.4 \pm 3.6\,\%$ was observed. The observed difference is well covered by a variation of $\pm 10\,\%$ quoted as the systematic error. Furthermore a small additional systematic uncertainty from a $\pm 20\,\%$ variation of the light quark charge tagging probabilities is included.

- The charm b tagging efficiency enters into the background subtraction via the flavour purities, in a similar way as the charm charge tagging probability. The charm background efficiency is subject to the tuning of the impact parameter resolution and to the Neural Net 'quality' information described above. Furthermore the modelling of charm events in the simulation affects the tagging rates, as will be discussed later in this section.

  It has been noticed that the charge and the b tagging are highly correlated and that both are sensitive to the quality of the tuning of the detector resolution for the background events. Therefore it is desirable to measure the charm efficiency directly from data. Preliminary studies using a double hemisphere tagging technique yield that the charm efficiency for different bins in b_{tag} is reproduced by the simulation to a level better than $20\,\%$. Reflecting the preliminary nature of this study, the $20\,\%$ uncertainty is used as an estimator for the systematic error assigned to the charm efficiency on top of the resolution and modelling errors. In the forward region an additional uncertainty is taken into account reflecting the reduced control over the sample near the edge of the Vertex Detector.

  It is expected that these systematic uncertainties will be reduced for the final publication.

- The hemisphere correlations are an important source of systematic uncertainty. The hemisphere charge correlations δ and β for this measurement are introduced by the jet charge as discussed in section 4.4. In reference [2] the hemisphere correlation for the jet charge at different values of κ have been measured from the data. Comparing the results to the simulation an uncertainty of $\pm 20\,\%$ was assigned to the scale of the correlation.

  For the measurement discussed here the size of the hemisphere correlation is given by the relative weight of the jet charge and the vertex based charge information. This variation is explicitly allowed for using intervals in b_{tag}, as for high values of b_{tag} good vertexing information is present in the event and consequently the hemisphere correlations are small.

- Hadronic interactions on average produce a positive charge in the event. This effect was studied in data and in simulation on the basis of the relative rate of positive charge double like-sign to negative charge double like-sign events. Reasonable agreement within errors was obtained between data and simulation. The influence on the measurement was found to be negligible.

- Even though in this measurement the bottom charge tagging probability is calibrated on data and the b efficiency is extracted assuming only efficiencies for background events, a residual sensitivity to the modelling of bottom fragmentation in

the simulation is introduced via the correlation of the b tagging and the size of the hemisphere correlations.

The fraction of different b hadron species in b events and their lifetimes as listed in table 6 are taken from reference [14]. The simulation was reweighted to reproduce the central values and a variation within the given error is included in the systematic error table. The average scaled energy $\langle x_E \rangle_b = 0.702 \pm 0.008$ per b hadron is taken from reference [15] and varied accordingly.

b hadron	fraction	lifetime [ps]
B^0	0.399 ± 0.011	1.546 ± 0.021
B^+	0.399 ± 0.011	1.647 ± 0.021
B_s	0.098 ± 0.012	1.464 ± 0.057
b baryons	0.103 ± 0.018	1.208 ± 0.051

Table 6: The fractions of particles produced in $Z \rightarrow b\overline{b}$ decays and their lifetimes [14].

- The modelling of charm production and decay properties affects directly the charm background subtraction in the measurement. As for the bottom events, the simulation is corrected to reproduce the charmed hadron fractions [10] and the their life times [17]. The values are listed in table 7. Following the prescription in reference [15] the rates of D^+, D_s and c baryons per c quark are varied individually. The changes are compensated by a shift of the D^0 fraction. The c hadron lifetimes are varied within the errors given.

  The influence of the uncertainty of the average scaled momentum fraction $\langle x_E \rangle$ of c hadrons in c events is studied by reweighting the events such that the resulting $\langle x_E \rangle$ changes corresponding to the uncertainty of the measurement $\langle x_E \rangle_c = 0.480 \pm 0.008$ [15].

charmed hadron	fraction	lifetime [ps]
D^0	0.541	0.415 ± 0.004
D^+	0.233 ± 0.016	1.057 ± 0.015
D_s	0.130 ± 0.027	0.447 ± 0.017
c baryons	0.096 ± 0.023	0.206 ± 0.012

Table 7: The fractions of particles produced in $Z \rightarrow c\overline{c}$ decays [10] and their lifetimes [17].

- The charge and the b tagging performance on charm events is dependent on the secondary vertex multiplicity. The inclusive branching ratios for D^+, D^0 and D_s into n, $n+2$ etc. charged particles have been measured by MARK III [17]. These branching ratios have been varied independently to determine the effect on the charm background correction. The systematic error assigned is the quadratic sum of all contributions.

- In light quark events a gluon splitting into a $c\overline{c}$ pair or $b\overline{b}$ pair gives rise to lifetime information from the decays of the produced heavy quark hadrons. A variation of

the splitting rates within the present world averages $g \to c\overline{c} = (2.96 \pm 0.38)\,\%$ and $g \to b\overline{b} = (0.254 \pm 0.051)\,\%$ [16] is included in the systematic error.

- Decays of K^0 and Λ in flight lead to tracks with large impact parameters with respect to the primary vertex and consequently can lead to a lifetime information in the event. The rate of such decays in light quark events was varied by $\pm 10\%$ to estimate the effect on the light quark efficiency ϵ_{uds} .

- The size of the QCD correction is theoretically known to be 0.0354 ± 0.0063 [12]. The experimental bias of the full analysis on the QCD correction has been discussed in section 5.1. Therefore the systematic uncertainty due to the QCD correction receives two contributions, one given by the statistical precision with which the QCD bias was estimated on simulation, the other one is given by the theoretical error multiplied by the experimental bias.

  In figure 6 the hemisphere correlations β and δ are shown with and without applying a cut of thrust$>$0.9. The differences are due to effects from gluon radiation. Hence the correction for the hemisphere correlations includes an implicit QCD correction. From the variation of the hemisphere correlation as a function of the thrust cut the bias on the QCD correction from hemisphere correlations is estimated to be 50 %. This additional bias factor has to be taken into account for the systematic error due to the theoretical uncertainty, adding 0.00030 to the value obtained from the study discussed before.

- The contribution to the total error due the limited Monte Carlo sample size can be estimated by dropping from the χ^2-fit the statistical uncertainties from the simulation. It is quoted separately from the pure statistical error of the data.

All contributions to the systematic error are summarised in Table 8.

Contribution	Variation	$\Delta A_{FB}^{\mathrm{b}} \times 10^2$
		92-95
R_{b}	0.21644 ± 0.00068	± 0.0002
R_{c}	0.1731 ± 0.0032	± 0.0011
A_{FB}^{c}	0.0689 ± 0.0035	± 0.014
detector resolution	see text	± 0.056
tuning of flavour tag	$\pm 50\,\%$	± 0.015
c (and uds) charge separation	$\pm 10\,\%(\pm 20\,\%)$	± 0.045
charm efficiency	see text	± 0.154
hemisphere correlations	$\pm 20\,\%$	∓ 0.120
B fractions in b events	see text	± 0.008
b hadron lifetimes	see text	± 0.006
average $x_E(b)$ in b events	0.702 ± 0.008	∓ 0.019
faction of D^+ in c events	0.233 ± 016	∓ 0.0012
faction of D_s in c events	0.130 ± 027	∓ 0.0054
faction of c baryons in c events	0.096 ± 0.023	± 0.0053
c hadron lifetimes	see text	± 0.007
average $x_E(c)$ in c events	0.484 ± 0.008	± 0.007
D charged decay multiplicities	see text	± 0.012
gluon splitting $g \to bb$	0.00235 ± 0.00051	± 0.001
gluon splitting $g \to c\bar{c}$	0.0296 ± 0.0038	< 0.0001
rate of K^0/Λ	$\pm 10\,\%$	± 0.003
error on QCD bias	see text	± 0.014
uncertainty of QCD correction	see text	± 0.040
statistical error of simulation		± 0.020
total systematic error		± 0.21

Table 8: Systematic uncertainties and their influence on the determination of A_{FB}^{b}.

7 Conclusions

This measurement of A_{FB}^{b}uses an enhanced impact parameter b tagging and an inclusive quark flavour tagging Neural Network. The analysis is based on the LEP 1 data collected with the DELPHI detector from 1992 up to 1995. The measured b quark forward-backward asymmetries for the individual years of data taking are:

$$\begin{array}{lrcl} 1992\ (91.280\ \mathrm{GeV}): & A_{FB}^{\mathrm{b}} & = & 0.1008 \pm 0.0082(\mathrm{stat.}) \\ 1993\ (91.225\ \mathrm{GeV}): & A_{FB}^{\mathrm{b}} & = & 0.1027 \pm 0.0099(\mathrm{stat.}) \\ 1994\ (91.202\ \mathrm{GeV}): & A_{FB}^{\mathrm{b}} & = & 0.0959 \pm 0.0049(\mathrm{stat.}) \\ 1995\ (91.288\ \mathrm{GeV}): & A_{FB}^{\mathrm{b}} & = & 0.0910 \pm 0.0087(\mathrm{stat.}) \end{array}$$

These measurements are QCD corrected. The final result is obtained taking correlated systematic errors into account:

$$A_{FB}^{\mathrm{b}}(91.234\ \mathrm{GeV}) \quad = \quad 0.0967 \pm 0.0036(\mathrm{stat.}) \pm 0.0021(\mathrm{syst.}) \quad .$$

From this measurement the b quark pole asymmetry is extracted. Corrections for QED, photon exchange and γZ interference amount to 0.0041 and -0.0003, respectively. A correction of -0.0008 is applied to correct for the energy dependence of the asymmetry. This yields:

$$A_{FB}^{0,\mathrm{b}} \quad = \quad 0.0997 \pm 0.0036(\mathrm{stat.}) \pm 0.0021(\mathrm{syst.}) \quad .$$

The measurement presented in this paper agrees well with previous determinations of $A_{FB}^{0,\mathrm{b}}$ at LEP and consequently with the LEP average value [10]. It improves by 25% on the precision with respect to the previous DELPHI results.

Acknowledgements

We are greatly indebted to our technical collaborators, to the members of the CERN-SL Division for the excellent performance of the LEP collider and to the funding agencies for their support in building and operating the DELPHI detector.
We acknowledge in particular the support of
Austrian Federal Ministry of Education, Science and Culture, GZ 616.364/2-III/2a/98,
FNRS–FWO, Flanders Institute to encourage scientific and technological research in the industry (IWT), Belgium,
FINEP, CNPq, CAPES, FUJB and FAPERJ, Brazil,
Czech Ministry of Industry and Trade, GA CR 202/96/0450 and GA AVCR A1010521,
Commission of the European Communities (DG XII),
Direction des Sciences de la Matière, CEA, France,
Bundesministerium für Bildung, Wissenschaft, Forschung und Technologie, Germany,
General Secretariat for Research and Technology, Greece,
National Science Foundation (NWO) and Foundation for Research on Matter (FOM), The Netherlands,
Norwegian Research Council,
State Committee for Scientific Research, Poland, 2P03B06015, 2P03B11116 and SPUB/P03/DZ3/99,
JNICT–Junta Nacional de Investigação Científica e Tecnológica, Portugal,
Vedecka grantova agentura MS SR, Slovakia, Nr. 95/5195/134,
Ministry of Science and Technology of the Republic of Slovenia,
CICYT, Spain, AEN96–1661 and AEN96-1681,
The Swedish Natural Science Research Council,
Particle Physics and Astronomy Research Council, UK,
Department of Energy, USA, DE–FG02–94ER40817.

Appendix

In this measurement events are sorted into five different categories. These categories are defined in section 4.2:

N	$\sim$	number of single hemisphere tagged forward events,
$\overline{N}$	$\sim$	number of single hemisphere tagged backward events,
N^D	$\sim$	number of double hemisphere tagged forward events,
$\overline{N^D}$	$\sim$	number of double hemisphere tagged backward events,
N^{same}	$\sim$	number of double tagged like-sign events.

w_f and w_f^D are the probabilities to identify the quark charge correctly in single and double tagged events. For single tagged events it is defined as:

$$w_\mathrm{f} = \frac{\hat{N}_\mathrm{f} + \hat{N}_{\overline{\mathrm{f}}}}{N_\mathrm{f} + N_{\overline{\mathrm{f}}}} \ , \tag{22}$$

where $N_\mathrm{f}(N_{\overline{\mathrm{f}}})$ is the number of events, which contain a quark (anti-quark) in the forward hemisphere. $\hat{N}_\mathrm{f}(\hat{N}_{\overline{\mathrm{f}}})$ is the number of events, in which the quark (anti-quark) has been correctly identified.

For unlike-sign events the fraction of events, in which both quark and anti-quark charges are correctly identified, is defined analogously to the single hemisphere tagged events as the ratio of correctly tagged $(\hat{N}_\mathrm{f}^D, \hat{N}_{\overline{\mathrm{f}}}^D)$ over all double-tagged unlike-sign $(N_\mathrm{f}^D, N_{\overline{\mathrm{f}}}^D)$ events:

$$w_\mathrm{f}^D = \frac{\hat{N}_\mathrm{f}^D + \hat{N}_{\overline{\mathrm{f}}}^D}{N_\mathrm{f}^D + N_{\overline{\mathrm{f}}}^D} \ . \tag{23}$$

The single and double tagged unlike- and like-sign samples receive contributions from b events and from all other flavours. All categories also include events for which the quark charge was misidentified. Therefore the number of events entering in the different categories can be expressed as:

$$N = \sum_{\mathrm{f=d,s,b}} [N_\mathrm{f} \cdot w_\mathrm{f} + N_{\overline{\mathrm{f}}} \cdot (1 - w_\mathrm{f})] + \sum_{\mathrm{f=u,c}} [N_{\overline{\mathrm{f}}} \cdot w_\mathrm{f} + N_\mathrm{f} \cdot (1 - w_\mathrm{f})] \tag{24}$$

$$\overline{N} = \sum_{\mathrm{f=d,s,b}} [N_{\overline{\mathrm{f}}} \cdot w_\mathrm{f} + N_\mathrm{f} \cdot (1 - w_\mathrm{f})] + \sum_{\mathrm{f=u,c}} [N_\mathrm{f} \cdot w_\mathrm{f} + N_{\overline{\mathrm{f}}} \cdot (1 - w_\mathrm{f})] \tag{25}$$

$$N^D = \sum_{\mathrm{f=d,s,b}} [N_\mathrm{f}^D \cdot w_\mathrm{f}^D + N_{\overline{\mathrm{f}}}^D \cdot (1 - w_\mathrm{f}^D)] + \sum_{\mathrm{f=u,c}} [N_{\overline{\mathrm{f}}}^D \cdot w_\mathrm{f}^D + N_\mathrm{f}^D \cdot (1 - w_\mathrm{f}^D)] \tag{26}$$

$$\overline{N^D} = \sum_{\mathrm{f=d,s,b}} [N_{\overline{\mathrm{f}}}^D \cdot w_\mathrm{f}^D + N_\mathrm{f}^D \cdot (1 - w_\mathrm{f}^D)] + \sum_{\mathrm{f=u,c}} [N_\mathrm{f}^D \cdot w_\mathrm{f}^D + N_{\overline{\mathrm{f}}}^D \cdot (1 - w_\mathrm{f}^D)] \tag{27}$$

$$N^{same} = \sum_{\mathrm{f=d,u,s,c,b}} N_\mathrm{f}^{same} \tag{28}$$

Here N_f $(N_{\overline{\mathrm{f}}})$ denominates the number of single tagged events containing a quark (anti-quark) of flavour f in the forward hemisphere. Similarly N_f^D $(N_{\overline{\mathrm{f}}}^D)$ is the number of

unlike-sign double tagged events containing a quark (anti-quark) of flavour f in the forward hemisphere. N_{f}^{same} is the number of like-sign double tagged events for each flavour.

Assuming a data sample which contains only b quark events, w_{b} can be extracted from the double tagged event samples. The sum of the unlike-sign double tagged events and the number of like-sign events is related to w_{b}:

$$N^D + \overline{N^D} = \left(N^D + \overline{N^D} + N^{same}\right) \cdot [w_{\mathrm{b}}^2 + (1 - w_{\mathrm{b}})^2] \quad (29)$$

$$N^{same} = 2 \cdot \left(N^D + \overline{N^D} + N^{same}\right) \cdot w_{\mathrm{b}} \cdot (1 - w_{\mathrm{b}}) \quad (30)$$

Both equations are linked through the total number of double tagged events and therefore contain the same information. Resolving the quadratic equation leads to the physical solution:

$$w_{\mathrm{b}} = \frac{1}{2} + \sqrt{\frac{1}{4} - \frac{1}{2} \cdot \frac{N^{same}}{N^D + \overline{N^D} + N^{same}}} \quad (31)$$

The second solution, with the minus sign, always leads to w_{b} values below 0.5.

The probability to identify a quark correctly for the single tag data sample can be used to calculate the probability to identify a quark or anti-quark correctly for the double tag data sample:

$$w_{\mathrm{b}}^D = \frac{w_{\mathrm{b}}^2}{w_{\mathrm{b}}^2 + (1 - w_{\mathrm{b}})^2} \quad (32)$$

Hemisphere charge correlations in the events entering the different categories need to be taken into account. For the probability w_{b} for single tagged events these correlations are given by term $\sqrt{1+\delta}$ which is introduced in Equation 31:

$$w_{\mathrm{b}} \cdot \sqrt{1+\delta} = \frac{1}{2} + \sqrt{\frac{1}{4} - \frac{1}{2} \cdot \frac{N^{same}}{N^D + \overline{N^D} + N^{same}}} \quad (33)$$

A similar correlation term, $\sqrt{1+\beta}$, has to be applied for the probability of the double tagged sample, w_{b}^D:

$$w_{\mathrm{b}}^D \cdot \sqrt{1+\beta} = \frac{{w_{\mathrm{b}}}^2 \cdot (1+\delta)}{{w_{\mathrm{b}}}^2 \cdot (1+\delta) + (1 - w_{\mathrm{b}} \cdot \sqrt{1+\delta})^2} \quad (34)$$

A last modification is needed because the selected double tagged data samples contain light and charm quark events in addition to the b quark events. The background events are taken into account by multiplying the different double tagged rates with the corresponding b purities:

$$w_{\mathrm{b}} \cdot \sqrt{1+\delta} = \frac{1}{2} + \sqrt{\frac{1}{4} - \frac{1}{2} \cdot \frac{N^{same} \cdot p_{\mathrm{b}}^{same}}{[N^D + \overline{N^D}] \cdot p_{\mathrm{b}}^D + N^{same} \cdot p_{\mathrm{b}}^{same}}} \quad (35)$$

Equation 34 is left unchanged. Equations 35 and 34 are used to extract the flavour tagging probability to measure the b quark forward-backward asymmetry.

References

[1] G.Altarelli et al., *Z PHYSICS AT LEP 1*, CERN 89-08 Volume 1, Geneva 1989.

[2] DELPHI Collaboration, P. Abreu et al., Eur. Phys. J. **C9** (1999) 367.

[3] DELPHI Collaboration, P. Antilogous et al., DELPHI 2000-101 CONF 400, contributed paper 377 to ICHEP2000, Osaka 2000.

[4] DELPHI Collaboration, P.Aarnio et al., Nucl. Instr. Meth. **A303** (1991) 233; DELPHI Collaboration, P.Abreu et al., Nucl. Instr. Meth. **A378** (1996) 57.

[5] T. Sjostrand, P. Eden, C. Friberg, L. Lonnblad, G. Miu, S. Mrenna and E. Norrbin, hep-ph/0010017.

[6] DELPHI Collaboration,P. Abreu et al. Z. Phys. **C73** (1996) 11.

[7] G.Borisov, C.Mariotti, Nucl. Instr. Meth. **A372** (1996) 181.

[8] DELPHI Collaboration, P.Abreu et al., Eur. Phys. J. **C10** (1999) 415.

[9] T. Allmendinger, G. Barker, M. Feindt, C. Haag, M. Moch, hep-ex/0102001.

[10] The LEP Collaborations, *A Combination of Preliminary Electroweak Measurements and Constraints on the Standard Model*, LEPEWWG/2001-01, Geneva 2001.

[11] D.Abbaneo et al., *QCD corrections to the forward-backward asymmetries of c and b quarks at the Z pole*, Eur. Phys. J. **C4** (1998) 185.

[12] The LEP Collaborations, *A Combination of Preliminary Electroweak Measurements and Constraints on the Standard Model*, CERN-EP/2000-016, Geneva 2000.

[13] DELPHI Collaboration, P.Abreu et al., Eur. Phys. J. **C10** (1999) 219.

[14] The LEP, SLD and CDF Collaborations, *Combined results on b-hadron production rates and decay properties*, CERN-EP in preparation.

[15] The LEP Heavy Flavour Group, *Input Parameters for the LEP/SLD Electroweak Heavy Flavour Results for Summer 1998 Conferences*, LEPHF/98-01.

[16] Klaus Mönig, private communication, average to be published in Summer 2001 issue of the LEP electroweak working group paper.

[17] MARK III Collaboration, D. Coffman et al., Phys. Lett. **B263** (1991) 135.